

---

# einspace: Searching for Neural Architectures from Fundamental Operations

---

Linus Ericsson<sup>1\*</sup> Miguel Espinosa<sup>1</sup> Chenhongyi Yang<sup>1</sup> Antreas Antoniou<sup>2</sup>  
 Amos Storkey<sup>2</sup> Shay B. Cohen<sup>2</sup> Steven McDonagh<sup>1</sup> Elliot J. Crowley<sup>1</sup>

<sup>1</sup> School of Engineering <sup>2</sup> School of Informatics  
 University of Edinburgh

Project page: <https://linusericsson.github.io/einspace>  
 Code: <https://github.com/linusericsson/einspace>



## Abstract

Neural architecture search (NAS) finds high performing networks for a given task. Yet the results of NAS are fairly prosaic; they did not e.g. create a shift from convolutional structures to transformers. This is not least because the search spaces in NAS often aren't diverse enough to include such transformations *a priori*. Instead, for NAS to provide greater potential for fundamental design shifts, we need a novel expressive search space design which is built from more fundamental operations. To this end, we introduce **einspace**, a search space based on a parameterised probabilistic context-free grammar. Our space is versatile, supporting architectures of various sizes and complexities, while also containing diverse network operations which allow it to model convolutions, attention components and more. It contains many existing competitive architectures, and provides flexibility for discovering new ones. Using this search space, we perform experiments to find novel architectures as well as improvements on existing ones on the diverse Unseen NAS datasets. We show that competitive architectures can be obtained by searching from scratch, and we consistently find large improvements when initialising the search with strong baselines. We believe that this work is an important advancement towards a transformative NAS paradigm where search space expressivity and strategic search initialisation play key roles.

## 1 Introduction

The goal of neural architecture search (NAS) [14, 41] is to automatically choose a network architecture for a given task, removing the need for expensive human expertise. NAS uses (i) a defined search space of all possible architectures that can be chosen, and (ii) a search algorithm e.g. [66, 56, 39] to navigate through the space, selecting the most suitable architecture with respect to search objectives. Despite significant research investment in NAS, with over 1000 papers released since 2020 [57], manually designed architectures still dominate the landscape. If someone looks through recent deep learning papers, they will most likely come across a (manually designed) transformer [54], or perhaps a (manually designed) MLP-Mixer [51], or even a (manually designed) ResNet [19]. Why isn't NAS being used instead?

---

\*linus.ericsson@ed.ac.uk

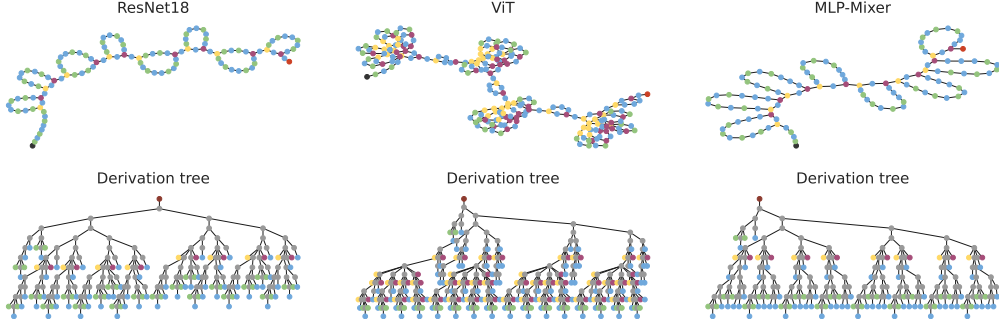


Figure 1: Three state-of-the-art architectures and their associated derivation trees within `einspace`. Top row shows the architectures where the black node is the input tensor and the red is the output. Bottom row shows derivation trees where the top node represents the starting symbol, the grey internal nodes the non-terminals and the leaf nodes the terminal operations. See Section 3.1 for details on other node colouring. Best viewed with digital zoom.

Part of the problem is that most NAS search spaces are not expressive enough, relying heavily on high-level operations and rigid structures. For example, in the DARTS [29] search space, each architecture consists of repeating cells; each cell is a directed acyclic graph where nodes are hidden states, and edges are operations drawn from a fixed set of mostly convolutions. This encodes a very specific prior—*architectures contain convolutions with multi-scale, filter-like structures* [48]—making it impossible to discover anything beyond ConvNet characteristics. Indeed, random search [61, 26] is often a strong baseline in NAS; networks sampled from unexpressive spaces behave very similarly [55] which makes it hard to justify an (often quite expensive) search.

One solution to this is to take the *ex nihilo* approach to search space construction. In AutoML-Zero [40] the authors create a very expressive search space that composes basic mathematical operations without any additional priors. However, searching through this space is far too expensive for mainstream use, requiring several thousand CPUs across several days to (re)discover simple operations like linear layers and ReLUs. Recent interest in hierarchical search spaces [45] has enabled the study of search across architecture granularities which naturally allows for greater flexibility. However, attempts so far have been limited to single architecture families like ConvNets [45] or transformers [65]. The hybrid search spaces that do exist have limited options both on the operation-level and macro structure [25, 59].

For NAS to be widely used we need the best of both worlds: a search space that is both highly expressive, and in which we can straightforwardly use existing tried-and-tested architectures as powerful priors for search. To this end, we propose `einspace`: a neural architecture search space based on a parameterised probabilistic context-free grammar (CFG). It is *highly expressive*, able to represent diverse network widths and depths as well as macro and micro structures. With its expressivity, the space contains disparate state-of-the-art architectures such as ResNets [19], transformers [54, 13] and the MLP-Mixer [51], as shown in Figure 1. Other notable architectures contained in `einspace` are DenseNet [23], WideResNet (WRN) [62], ResMLP [52] and the Vision Permutator [21].

We realise our proposed search space through the creation of function-mapping groups that define a broad class of fundamental network operations and further describe how such elements can be composed into full architectures under the natural recursive capabilities of our CFG. To guarantee the validity of all architectures generated within the expressive space, we first extend our base CFG with parameters that ensure diverse components can be combined into complex structures. Next, we balance the contention between search space *flexibility* and search space *complexity* by introducing mild constraints on our search space via branching and symmetry-based priors. Finally, we integrate probabilities into our production rules to further control the complexity of architectures sampled from our space.

To demonstrate the effectiveness of `einspace`, we perform experiments on the Unseen NAS datasets [16]—eight diverse classification tasks including vision, language, audio, and chess problems—using simple random and evolutionary search strategies. We find that in such an expressive search space, the choice of search strategy is important and random search underperforms. When using the powerful priors of human-designed architectures to initialise the search, we consistently find

both large performance gains and significant architectural changes. Code to reproduce our experiments is available at <https://github.com/linusericsson/einspace>.

Using only simple search strategies, we can still identify competitive architectures, indicating that further refining these strategies in `einspace` could lead to significant advancements. We hope that this novel perspective on search spaces—focusing on expressiveness and incorporating the priors of existing state-of-the-art architectures—has the potential to drive NAS research towards a new paradigm.

## 2 Background

### Neural architecture search

The search space used in NAS has a significant impact on results [61, 63]. This has facilitated the need to investigate search space design alongside the actual search algorithms [36]. Early macro design spaces [24, 66] made use of naive building blocks while accounting for skip connections and branching layers. Further design strategies have looked at chain-structured [3, 4, 6, 42], cell-based [67, 64, 29, 15] and hierarchical approaches. Hierarchical search spaces have been shown to be expressive and effective in reducing search complexity and methods include factorised approaches [50],  $n$ -level hierarchical assembly [27, 28, 46], parameterisation of hierarchical random graph generators [44] and topological evolutionary strategies [34]. Additional work on search spaces have proposed new candidate operations and module designs such as hand-crafted multi-branch cells [49], tree-structures [3], shuffle operations [31], dynamic modules [22], activation functions [37] and evolutionary operators [10]. In AutoML-Zero [40], the authors try to remove human bias from search space construction by defining a space of basic mathematical operations as building blocks.

The pioneering work of [45] constructs search spaces using CFGs. We take this direction further and construct `einspace` as a probabilistic CFG allowing for unbounded derivations, balanced by careful tuning of the branching rate. We aim to strike a balance of the level of complexity in the search space while incorporating components from diverse state-of-the-art architectures. Crucially, our space enables flexibility in both macro structure and at the individual operation level. While previous search spaces can be instantiated for specific architecture classes, our single space incorporates multiple classes in one, ConvNets, transformers and MLP-only architectures. Such hybrid spaces have been explored before [25], but they have been limited in their flexibility, offering only direct choices between convolution and attention operations and not allowing the construction of novel components.

Prominent search strategies include Bayesian optimisation [33, 56], reinforcement learning [64, 66, 67] and genetic algorithms [5, 38, 39]. A popular thread of work, towards improving computational efficiency via amortising training cost, involves the sharing of weights between different architectures via a supernet [1, 3, 9, 18, 29, 30]. Efficiency has been further improved by sampling only a subset of supernet channels [58], thus reducing both space exploration redundancies and memory consumption. Alternative routes to mitigating space requirements have considered both architecture and operation-choice pruning [7, 15]. We however highlight that random search often proves to be a very strong baseline [26, 61]; a consequence of searching within narrow spaces. This is commonly the case for highly engineered search spaces that contain a high fraction of strong architectures [57]. Contrasting this, in our `einspace` we see that random search across many tasks performs poorly, underpinning the value of a good search strategy for large, diverse search spaces [2, 40].

### Context-free grammars

A context-free grammar (CFG; [20]) is a tuple  $(N, \Sigma, R, S)$ , where  $N$  is a finite set of *non-terminal* symbols,  $\Sigma$  is a finite set of *terminal* symbols,  $R$  is the set of *production rules*—where each rule maps a non-terminal  $A \in N$  to a string of non-terminal or terminals  $A \rightarrow (N \cup \Sigma)^+$ —and  $S$  is the *starting symbol*. A CFG describes a context-free language, containing all the strings that the CFG can generate. By recursively selecting a production, starting with the rules containing the starting symbol, we can generate strings within the grammar. CFGs can be *parameterised*: each non-terminal, in each rule in  $R$ , is annotated with parameters  $p_1, \dots, p_n$  that influence the production (right hand side parameters have to appear in the left hand side). These parameters can condition production, based on an external state or contextual information, thus extending the power of the grammar.

A *probabilistic* context-free grammar (PCFG) associates each production rule with a probability [32]. These define the likelihood of selecting a particular rule given a parent non-terminal. These probabilities allow for stochastic string generation.

### 3 einspace: A Search Space of Fundamental Operations

Our neural architecture search space, `einspace`<sup>2</sup> is introduced here. Based on a parameterised PCFG, it provides an expressive space containing many state-of-the-art neural architectures. We first describe the groups of operations we include in the space, then how macro structures are represented. We then present the CFG that defines the search space and its parameterised and probabilistic extensions.

As a running example we will be constructing a simple convolutional block with a skip connection within `einspace`, explaining at each stage how it relates to the architecture. The block will consist of a convolution, a normalisation and an activation, wrapped inside a skip connection.

#### 3.1 Fundamental Operations

Each fundamental operation within `einspace` takes as input a tensor, either the tensor that is passed as input to the whole network or a tensor from a previous operation, and operates on it further. An operation can be thought of as a *layer* in a processing pipeline that defines the overall network. The fundamental operations can be separated into four groups of functions that define their role in a network architecture. The terms one-to-one, one-to-many and many-to-one below refer to the number of input and output tensors of the functions within that group. For full details of the operations, see Appendix A.2

**Branching.** *One-to-many* functions that direct the flow of information through the network by cloning or splitting tensors. Examples include the branching within self-attention modules into queries, keys and values. In our visualisations, these are coloured **yellow**.

**Aggregation.** *Many-to-one* functions that merge the information from multiple tensors into one. Examples include matrix multiplication, summation and concatenation. In our visualisations, these are coloured **purple**.

**Routing.** *One-to-one* functions that change the shape or the order of the content in a tensor without altering its information. Examples include axis permutations as well as the `im2col` and `col2im` operations. In our visualisations, these are coloured **green**.

**Computation.** *One-to-one* functions that alter the information of the tensor, either by parameterised operations, normalisation or non-linearities. Examples include linear layers, batch norm and activations like ReLU and softmax. In visualisations, these are coloured **blue**.

In our example, the skip connection will be handled by a combination of branching and aggregation functions, the convolution is decomposed into the routing functions `im2col` and `col2im`, with a linear layer from the computation group between them. The normalisation and activation come from the computation group. In the next subsection, we discuss the larger structures of the architecture.

#### 3.2 Macro Structure

The groups of functions above describe the fundamental operations that make up an architecture. We now describe how these functions are composed in different ways to form larger components.

A *module* is defined as a composition of functions from above that takes one input tensor and produces one output tensor, with potential branching inside. A module may contain multiple *computation* and *routing* operations, but each *branching* must be paired with a subsequent *aggregation* operation. Thus, the whole network can be seen as a module that takes a single tensor as input and outputs a single prediction. A network module may itself contain multiple modules, directly pertaining to the hierarchical phrase nature of CFG structures. We divide modules into four types, visualised in Figure 2.

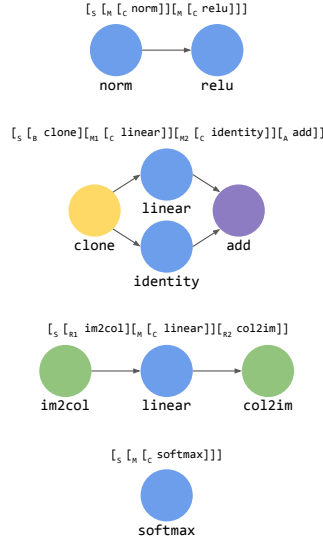


Figure 2: Visualisation of example modules with their CFG derivations in bracket notation. From top to bottom; sequential, branching, routing and computation modules.

<sup>2</sup>The name is inspired by the generality of the *Einstein summation* and related Python library `einops` [43] as many of our operations can be implemented in it.

**Sequential module.** A pair of modules and/or functions that are applied to the input tensor sequentially. Using our grammar, defined in Section 3.3, this can be produced using the rule ( $M \rightarrow MM$ ), or equivalently from the starting symbol  $S$ . This also applies to the rules below.

**Branching module.** A branching function first splits the input into multiple branches. Each branch is processed by some inner set of modules and/or functions. The outputs of all branches are subsequently merged in an aggregation function. In the grammar below this can be produced by the rule ( $M \rightarrow BMA$ ).

**Routing module.** A routing function is applied, followed by a module and/or function. A final routing function then processes the output tensor. In the grammar below this is produced by the rule ( $M \rightarrow R1MR2$ ). For more details on the role of the routing module, see Appendix A.3.

**Computation module.** This module only contains a single function, selected from the one-to-one computation functions described above. While this module is trivial, we will see later how its inclusion is helpful when designing our CFG and its probabilistic extension. In the grammar below this is produced by the rule ( $M \rightarrow C$ ).

To construct our example, we will be using all four modules. The branching module combines the `clone` and `add` functions from before to create a 2-branch structure. One branch is a simple skip connection by using the `identity` function inside a computation module. The other branch is the more complex sequence. The convolutional layer is created by combining `im2col`, `linear` and `col2im` in a routing module. The norm and activation are each wrapped in a computation module and these are all composed in sequential modules. Figure 2 shows similar module instantiations in action.

### 3.3 Search Space as a Context-Free Grammar

The following CFG defines our `einspace`, where uppercase symbols represent non-terminals and lowercase represent terminals. The colours refer to the function groups.

```

S → M M | B M A | R1 M R2,
M → M M | B M A | R1 M R2 | C,
B → clone | group-dim,
A → matmul | add | concat,
R1 → identity | im2col | permute,
R2 → identity | col2im | permute,
C → identity | linear | norm | relu | softmax | pos-enc.

```

Our networks are all constructed according to the high-level blueprint: `backbone` → `head` where `head` is a predefined module that takes an output feature from the backbone and processes it into a prediction (see Appendix B for more details). The `backbone` is thus the section of the network that is generated by the above CFG. When searching for architectures we search across different backbones.

Completing our running example, we present the full derivation of the architecture in the CFG in Figure 3.

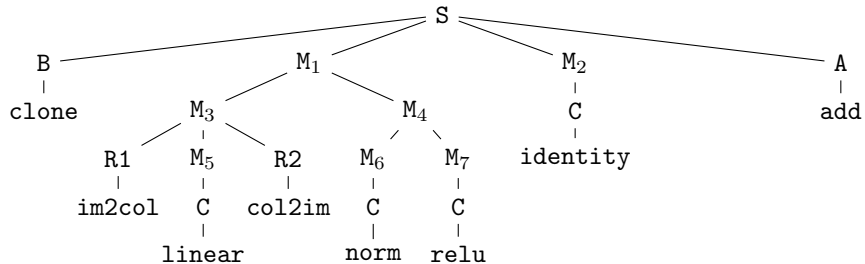


Figure 3: Example derivation tree of a traditional convolutional block with a skip connection.

### 3.4 Prior Choices

When designing a search space, we must balance the need for flexibility—which allows more valid architectures to be included—and constraints – which reduce the size of the search space. We can view constraints as imposing priors on which architectures we believe are worth including. As discussed, many previous frameworks are too restrictive; therefore, we aim to impose minimal priors, listed below.

**Convolutional prior.** We design our routing module to enable convolutions to be easily constructed, while also allowing components like patch embeddings and transpose operations. We thus enforce that a routing function is followed by another routing function later in the module. Moreover, `im2col` only appears in the production rule of the first routing function ( `R1` ) and `col2im` in the last ( `R2` ). As shown in Figure 2, to construct a convolution, we start from the rule (  $M \rightarrow R1 M R2$  ) and derive the following (  $R1 \rightarrow \text{im2col}$  ), (  $M \rightarrow C \rightarrow \text{linear}$  ) and (  $R2 \rightarrow \text{col2im}$  ).

**Branching prior.** We also impose a prior on the types of branching that can occur in a network. The branching functions `clone` and `group-dim` can each have a branching factor of 2, 4 or 8. For a factor of 2, we allow each inner function to be unique, processing the two branches in potentially different ways. For branching factors of 4 or 8, the inner function  $M$  is repeated as is, processing all branches identically (though all inner functions are always initialised with separate parameters). Symbolically, given a branching factor of 2 we have (  $BM_1 M_2 A$  ) but with a branching factor of 4 we have (  $BM_1 M_1 M_1 M_1 A$  ). Examples of components instantiated by a branching factor of 2 include skip connections, and for 4, or 8, multi-head attention.

### 3.5 Feature Mode

Different neural architectures operate on different feature shapes. ConvNets maintain 3D features throughout most of the network while transformers have 2D features. To enable such different types of computations in the same network, we introduce the concept of a *mode*<sup>3</sup> that affects the shape of our features and which operations are available at that point in the network. Before and after each module, we fix the feature tensor to be of one of two specific shapes, depending on which mode we are in.

**Im mode.** Maintains a 3D tensor of shape (  $C, H, W$  ), where  $C$  is the number of channels,  $H$  is the height and  $W$  is the width. Most convolutional architectures operate in this mode.

**Col mode.** Maintains a 2D tensor of shape (  $S, D$  ), where  $S$  is the sequence length and  $D$  is the token dimensionality. This is the mode in which most transformer architectures operate.

The mode is changed by the routing functions `im2col` and `col2im`. Most image datasets will provide inputs in the `Im` mode, while most tasks that use a language modality will provide it in `Col` mode.

Our example architecture maintains the `Im` mode at almost all stages, apart from inside the routing modules where the `im2col` function briefly puts us in the `Col` mode before `col2im` brings us back.

### 3.6 Parameterising the Grammar

Due to the relatively weak priors we have put on the search space, sampling a new architecture naively will often lead to invalid networks. For example, the shape of the output tensor of one operation may not match the expected input shape of the next. Alternatively, the branching factor of a branching function may not match the branching factor of its corresponding aggregation function.

We therefore extend the grammar with parameters. Each rule  $r$  now has an associated set of parameters (  $s, m, b$  ) which defines in what situations this rule can occur. When we sample an architecture from the grammar, we start by assigning parameter values based on the expected input to the architecture. For example, they might be the input tensor shape, feature mode and branching factor:

$$(s = [3, 224, 224], m = \text{Im}, b = 1). \quad (1)$$

Given this, we can continuously infer the current parameters during each stage of sampling by knowing how each operation changes them. When we expand a production rule, we must choose a rule which has matching parameters. If at some point, the sampling algorithm has no available valid options, it

---

<sup>3</sup>Note that this is similar but not the same as the *mode* of a general tensor, which determines the number of dimensions of that tensor. We use the term mode to refer to the state that a particular part of the architecture is in.

will backtrack and change the latest decision until a full valid architecture is found. Hence, we can ensure that we can sample architectures without risk of obtaining invalid ones.

As an example of this, the CFG rule for R1 was previously

$$R1 \rightarrow \text{identity} \mid \text{im2col} \mid \text{permute}. \quad (2)$$

Enhanced with parameters, this now becomes two rules

$$R1(m=\text{Im}) \rightarrow \text{identity} \mid \text{im2col} \mid \text{permute}, \quad (3)$$

$$R1(m=\text{Col}) \rightarrow \text{identity} \mid \text{permute}. \quad (4)$$

This signifies that an `col2im` operation is not available in the `Im` mode. Similarly, the available aggregation options depend on the branching factor of the current branching module

$$A(b=2) \rightarrow \text{matmul} \mid \text{add} \mid \text{concat}, \quad (5)$$

$$A(b=4) \rightarrow \text{add} \mid \text{concat}, \quad (6)$$

$$A(b=8) \rightarrow \text{add} \mid \text{concat}. \quad (7)$$

### 3.7 Balancing Architecture Complexity

When sampling an architecture, we construct a decision tree where non-leaf nodes represent decision points and leaf nodes represent architecture operations. In each iteration, we either select a non-terminal module to expand the architecture and continue sampling, or choose a terminal function to conclude the search at that depth. Continuously selecting modules results in a deeper, more complex network, whereas selecting functions leads to a shallower, simpler network. We can balance this complexity by assigning probabilities to our production rules, thereby making a PCFG. Recall our CFG rule

$$(M \rightarrow M M \mid B M A \mid R1 M R2 \mid C). \quad (8)$$

If we choose one of the first three options we are delving deeper in the search tree since there is yet another `M` to be expanded, but if we choose  $(M \rightarrow C)$ , the *computation-module*, then we will reach a terminal function. Thus, to balance the depth of our traversal and therefore expected architecture complexities, we can set probabilities for each of these rules:

$$p(M \rightarrow M M \mid M), \quad p(M \rightarrow B M A \mid M), \quad p(M \rightarrow R1 M R2 \mid M), \quad p(M \rightarrow C \mid M). \quad (9)$$

The value of  $p(M \rightarrow C \mid M)$  is especially important as it can be interpreted as the probability that we will stop extending the search tree at the current location.

We could set these probabilities to match what we wish the expected depth of architectures to be (for empirical results on the architecture complexity, see Table 6 in the Appendix). However, we can actually ensure that the CFG avoids generating infinitely long architecture strings by setting the probabilities such that the branching rate of the CFG is less than one [8]. For details of how, see Appendix A.4. So, as shown in Figure 4, we set the computation module probability to  $p(M \rightarrow C \mid M) = 0.32$  and the probabilities of the other modules to  $\frac{1-0.32}{3} = \frac{1}{3}$ . For simplicity, all other rule probabilities are uniform.

For a thorough example of how sampling is performed in `einspace`, please see Appendix A.1.

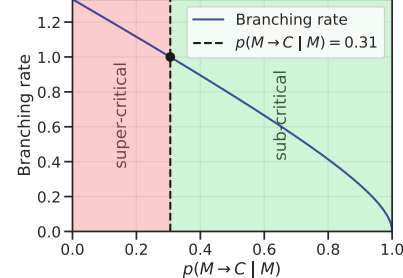


Figure 4: To ensure our CFG is consistent and does not generate infinite architectures, we make sure the branching rate is in the sub-critical region by setting  $p(M \rightarrow C \mid M) > 0.31$ .

## 4 Experiments

### 4.1 Experimental Details

#### Datasets

As our search space strives for expressivity and diverse architectures, we adopt a diverse benchmark

suite from the recent paper on Unseen NAS [16], containing datasets at different difficulties across vision, language, audio and further modalities. See Appendix B.2 for the detailed dataset descriptions.

While Unseen NAS forms the basis of this section, we run additional experiments on a selection of datasets from NAS-Bench-360 [53] in Appendix C.1, where we beat competing NAS methods on CIFAR100 and Darcy Flow, and to the best of our knowledge set a new state-of-the-art on NinaPro.

### Search strategy

We explore three search strategies within `einspace`: random sampling, random search, and regularised evolution (RE). *Random sampling* estimates the average expected test performance from  $K$  random architecture samples. *Random search* samples  $K$  architectures and selects the best performer on a validation set. In *regularised evolution*, we start by constructing an initial population of 100 individuals, which are either randomly sampled from the search space or seeded with existing architectures. For  $(K - 100)$  iterations, the algorithm then randomly samples 10 individuals and selects the one with the highest fitness as the parent. This parent is mutated to produce a new child. This child is evaluated and enters the population while the oldest individual in the population is removed, following a first-in-first-out queue structure. An architecture is mutated in three straightforward steps:

1. *Sample a Node*: Uniformly at random sample a node in the architecture derivation tree.
2. *Resample the Subtree*: Replace the subtree rooted at the sampled node by regenerating it based on the grammar rules. This step allows the exploration of new configurations, potentially altering a whole subtree if a non-leaf node is chosen.
3. *Validate Architecture*: Check if the new architecture can produce a valid output in the forward pass, given an input of the expected shape, and that it fits within resource constraints, e.g. GPU memory. If it does, accept it; otherwise, discard and retry the mutation.

Note that these are very simple search strategies, and that there is huge potential to design more intelligent approaches, e.g. including crossover operations in the evolutionary search, using hierarchical Bayesian optimisation [45] or directly learning the probabilities of the CFG [11]. In this work, we focus on the properties of our search space and investigate whether simple search strategies are able to find good architectures, and leave investigations on more complex search strategies for future work.

### Baselines

We compare these search strategies to PC-DARTS [58], DrNAS [7] and Bonsai-Net [15] with results transcribed from [16]. We also compare to the performance of a trained ResNet18 (RN18). More details on the baselines, training recipes and network instantiations can be found in Appendix B.1

## 4.2 Random Sampling and Search

In previous NAS search spaces e.g. [29, 60, 12], complex search methods often perform very similarly to random search [26, 61]. Indeed, we can see this in Table 1 comparing the PC-DARTS strategy to DARTS random search.

However for `einspace`, this is not the case for most datasets. Random sampling improves on pure random guessing (not shown), but is far from the baseline performance of a ResNet18. The random search baseline is also far behind, but intriguingly outperforms baseline NAS approaches on Chesseract.

## 4.3 Evolutionary Search from Scratch

We now turn to a more sophisticated search strategy. We perform regularised evolution in `einspace` for 1000 iterations across all datasets, initialising the population with 100 random samples. In Table 1 the results are shown in the column named RE(Scratch). The performance of this strategy is significantly higher than random search on several datasets, indicating that the search strategy is more important in an expressive search space like `einspace` compared to DARTS. Compared to the top performing NAS methods, however, it is significantly behind on some datasets.



Figure 5: The top RE(Mix) architecture on AddNIST, found in `einspace`.

Table 1: NAS performance resulting from the combination of `einspace` with the simple search strategies of random sampling, random search, and regularised evolution (RE). See text for further detail. We evaluate performance across multiple datasets and modalities from Unseen NAS [16]. Search space results transcribed from [16] are denoted <sup>\*</sup>, where DARTS [29] and Bonsai [15] search spaces are employed. The expressiveness of `einspace` enables performance that remains competitive with significantly more elaborate search strategies. **Best** and second best performance per dataset.

Dataset	Baselines				Regularised evolution (RE) <code>einspace</code>			Rand. Search		Rand. Sampl.	
	RN18	PC-DARTS <sup>*</sup>	Dr NAS <sup>*</sup>	Bonsai-Net <sup>*</sup>	RE (RN18)	RE (Mix)	RE (Scratch)	DARTS <sup>*</sup>	Bonsai <sup>*</sup>	ein space	ein space
AddNIST	93.36	96.60	97.06	<b>97.91</b>	97.54	97.72	83.87	97.07	34.17	67.00	10.13
Language	92.16	90.12	88.55	87.65	96.84	<b>97.92</b>	88.12	90.12	76.83	87.01	35.26
MultNIST	91.36	96.68	<b>98.10</b>	97.17	96.37	92.25	93.72	96.55	39.76	66.09	18.87
CIFARTile	47.13	<b>92.28</b>	81.08	91.47	60.65	62.76	30.89	90.74	24.76	30.90	25.25
Gutenberg	43.32	49.12	46.62	48.57	<b>54.02</b>	50.16	36.70	47.72	29.00	39.58	19.69
Isabella	63.65	65.77	64.53	64.08	64.30	62.72	56.33	<b>66.35</b>	58.53	56.90	32.24
GeoClassing	90.08	94.61	<b>96.03</b>	95.66	95.31	95.13	60.43	95.54	63.56	69.13	24.35
Chesseract	59.35	57.20	58.24	60.76	60.31	61.86	59.50	59.16	<b>68.83</b>	61.46	44.83
Average acc. $\uparrow$	72.55	80.30	78.78	<b>80.41</b>	78.17	77.56	63.70	<b>80.41</b>	49.43	59.76	26.32
Average rank $\downarrow$	6.50	4.44	4.38	<b>3.50</b>	3.75	3.88	8.12	4.06	8.62	7.88	10.88

#### 4.4 Evolutionary Search from Existing SOTA Architectures

To fully utilise the powerful priors of existing human-designed structures, we now search with the initial population of our evolutionary search seeded with a collection of existing state-of-the-art architectures.

We first seed the entire population with the ResNet18 architecture. The search applies mutations to these networks for 500 iterations. In Table 1, these results can be found in the RE(RN18) column.

To further highlight the expressivity of `einspace`, we perform experiments searching from an initial population seeded with a mix of ResNet18, WRN16-4, ViT and MLP-Mixer architectures. To our knowledge, no other NAS space is able to represent such a diverse set of architectures in a single space. These results are shown in the RE(Mix) column.

Overall, we find that on **every single task**, we can find an improved version of the initial architecture using RE(RN18) and on all but one using RE(Mix). Moreover, in some cases we can beat the existing state-of-the-art, especially on tasks further from the traditional computer vision setting. In particular, where previous NAS methods fail—i.e. the Language dataset—the architecture in Figure 6 has a direct improvement over the ResNet18 by 5.76%. See also the architecture in Figure 5 and the collection in Figure 8 in the Appendix for the breadth of structures that are found in `einspace`.

One dataset where our searches struggle is CIFARTile, a more complex version of the CIFAR10 dataset. While large improvements are made to the baseline networks, they still lag behind other NAS methods. This shows how the strong and restricted focus on ConvNets within the DARTS search space is highly successful for traditional computer vision style tasks that have been common in the literature.

## 5 Limitations

Our search space, designed for diversity, is extremely large and uniquely unbounded in terms of depth and width. This complexity makes formulating one-shot methods like ENAS [35] or DARTS [29] challenging. Instead, developing an algorithm to learn the probabilities of the PCFG may be more feasible. This approach, however, must address the grammar’s context-free nature where sampling

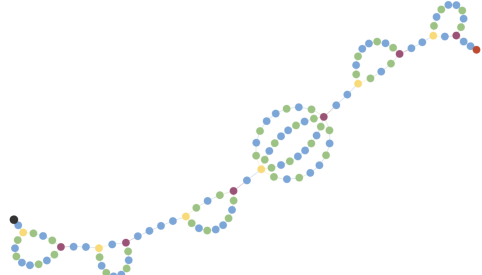


Figure 6: The best model on the Language dataset, found by RE(Mix) in `einspace`.

probabilities do not consider network depth, feature shape, or previous decisions, although this could be mitigated by using the parameters outlined in Section 3.6.

Another issue is ambiguity arising from the possibility of multiple derivation trees for a single architecture, primarily due to the multiple ways of stacking sequential modules. Moreover, we have found that through sampling and mutation, some architectures’ components reduce to the identity operation, from e.g. stacked identity and permute operations within sequential and routing modules.

Finally, we designed `einspace` to be diverse, but some key structures cannot be represented in its current form. There are no options for recurrent computation, as found in RNNs and the new wave of state-space models like Mamba [17]. We also chose to keep the options for activations and normalisation layers as small as possible since in practice the benefit from changing these is minor.

## 6 Conclusion

We have introduced `einspace`: an expressive NAS search space based on a parameterised PCFG. We show that our work enables the construction of a comprehensive and diverse range of existing state-of-the-art architectures and can further facilitate discovery of novel architectures directly from fundamental operations. With only simple search strategies, we report competitive resulting architectures across a diverse set of tasks, highlighting the potential value of defining highly expressive search spaces. We further demonstrate the utility of initialising search with existing architectures as priors. We believe that future work on developing intelligent search strategies within `einspace` can lead to exciting advancements in neural architectures.

## Acknowledgements and Disclosure of Funding

The authors are grateful to Joseph Mellor, Henry Gouk, and Thomas L. Lee for helpful suggestions. Funding for this research is provided by an EPSRC New Investigator Award (EP/X020703/1).

## References

- [1] Gabriel Bender, Pieter-Jan Kindermans, Barret Zoph, Vijay Vasudevan, and Quoc V Le. Understanding and simplifying one-shot architecture search. In *International Conference on Machine Learning*, 2018.
- [2] Gabriel Bender, Hanxiao Liu, Bo Chen, Grace Chu, Shuyang Cheng, Pieter-Jan Kindermans, and Quoc V Le. Can weight sharing outperform random architecture search? An investigation with tunas. In *Proceedings of the IEEE/CVF Conference on computer vision and pattern recognition*, 2020.
- [3] Han Cai, Ligeng Zhu, and Song Han. Proxylessnas: Direct neural architecture search on target task and hardware. In *International Conference on Learning Representations*, 2019.
- [4] Han Cai, Chuang Gan, Tianzhe Wang, Zhekai Zhang, and Song Han. Once-for-all: Train one network and specialize it for efficient deployment. In *International Conference on Learning Representations*, 2020.
- [5] Angelica Chen, David Dohan, and David So. Evoprompting: Language models for code-level neural architecture search. *Advances in Neural Information Processing Systems*, 2023.
- [6] Minghao Chen, Houwen Peng, Jianlong Fu, and Haibin Ling. Autoformer: Searching transformers for visual recognition. In *Proceedings of the IEEE/CVF International Conference on Computer Vision*, 2021.
- [7] Xiangning Chen, Ruochen Wang, Minhao Cheng, Xiaocheng Tang, and Cho-Jui Hsieh. DrNAS: Dirichlet neural architecture search. In *International Conference on Learning Representations*, 2020.
- [8] Zhiyi Chi. Statistical properties of probabilistic context-free grammars. *Computational Linguistics*, 25(1):131–160, 1999.

- [9] Xiangxiang Chu, Bo Zhang, and Ruijun Xu. FairNAS: Rethinking evaluation fairness of weight sharing neural architecture search. In *Proceedings of the IEEE/CVF International Conference on Computer Vision*, 2021.
- [10] Yuanzheng Ci, Chen Lin, Ming Sun, Boyu Chen, Hongwen Zhang, and Wanli Ouyang. Evolving search space for neural architecture search. In *Proceedings of the IEEE/CVF International Conference on Computer Vision*, 2021.
- [11] Shay Cohen. Latent-Variable PCFGs: Background and applications. In *Proceedings of the 15th Meeting on the Mathematics of Language*, 2017.
- [12] Xuanyi Dong and Yi Yang. Nas-bench-201: Extending the scope of reproducible neural architecture search. In *International Conference on Learning Representations*, 2019.
- [13] Alexey Dosovitskiy, Lucas Beyer, Alexander Kolesnikov, Dirk Weissenborn, Xiaohua Zhai, Thomas Unterthiner, Mostafa Dehghani, Matthias Minderer, Georg Heigold, Sylvain Gelly, Jakob Uszkoreit, and Neil Houlsby. An image is worth  $16 \times 16$  words: Transformers for image recognition at scale. In *International Conference on Learning Representations*, 2021.
- [14] Thomas Elsken, Jan Hendrik Metzen, and Frank Hutter. Neural architecture search: A survey. *Journal of Machine Learning Research*, 20(55):1–21, 2019.
- [15] Rob Gead, Dennis Prangle, and A Stephen McGough. Bonsai-net: One-shot neural architecture search via differentiable pruners. *arXiv preprint arXiv:2006.09264*, 2020.
- [16] Rob Gead, David Towers, Matthew Forshaw, Amir Atapour-Abarghouei, and A Stephen McGough. Insights from the use of previously unseen neural architecture search datasets. In *Proceedings of the IEEE/CVF Conference on Computer Vision and Pattern Recognition*, 2024.
- [17] Albert Gu and Tri Dao. Mamba: Linear-time sequence modeling with selective state spaces. *arXiv preprint arXiv:2312.00752*, 2023.
- [18] Zichao Guo, Xiangyu Zhang, Haoyuan Mu, Wen Heng, Zechun Liu, Yichen Wei, and Jian Sun. Single path one-shot neural architecture search with uniform sampling. In *Proceedings of the European Conference on Computer Vision*, 2020.
- [19] Kaiming He, Xiangyu Zhang, Shaoqing Ren, and Jian Sun. Deep residual learning for image recognition. In *Proceedings of the IEEE Conference on Computer Vision and Pattern Recognition*, 2016.
- [20] John E Hopcroft, Rajeev Motwani, and Jeffrey D Ullman. Introduction to automata theory, languages, and computation. *ACM SigAct News*, 32(1):60–65, 2001.
- [21] Qibin Hou, Zihang Jiang, Li Yuan, Ming-Ming Cheng, Shuicheng Yan, and Jiashi Feng. Vision permutator: A permutable MLP-like architecture for visual recognition. *IEEE Transactions on Pattern Analysis and Machine Intelligence*, 45(1):1328–1334, 2023.
- [22] Jie Hu, Li Shen, and Gang Sun. Squeeze-and-excitation networks. In *Proceedings of the IEEE/CVF Conference on Computer Vision and Pattern Recognition*, 2018.
- [23] Gao Huang, Zhuang Liu, Laurens van der Maaten, and Kilian Q Weinberger. Densely connected convolutional networks. In *Proceedings of the IEEE Conference on Computer Vision and Pattern Recognition*, 2017.
- [24] Kirthevasan Kandasamy, Willie Neiswanger, Jeff Schneider, Barnabas Poczos, and Eric P Xing. Neural architecture search with bayesian optimisation and optimal transport. *Advances in Neural Information Processing Systems*, 2018.
- [25] Changlin Li, Tao Tang, Guangrun Wang, Jiefeng Peng, Bing Wang, Xiaodan Liang, and Xiaojun Chang. BossNAS: Exploring hybrid CNN-transformers with block-wisely self-supervised neural architecture search. In *Proceedings of the IEEE/CVF International Conference on Computer Vision*, 2021.
- [26] Liam Li and Ameet Talwalkar. Random search and reproducibility for neural architecture search. In *Conference on Uncertainty in Artificial Intelligence*, 2019.

[27] Chenxi Liu, Liang-Chieh Chen, Florian Schroff, Hartwig Adam, Wei Hua, Alan L Yuille, and Li Fei-Fei. Auto-deeplab: Hierarchical neural architecture search for semantic image segmentation. In *Proceedings of the IEEE/CVF Conference on Computer Vision and Pattern Recognition*, 2019.

[28] Hanxiao Liu, Karen Simonyan, Oriol Vinyals, Chrisantha Fernando, and Koray Kavukcuoglu. Hierarchical representations for efficient architecture search. In *International Conference on Learning Representations*, 2018.

[29] Hanxiao Liu, Karen Simonyan, and Yiming Yang. DARTS: Differentiable architecture search. In *International Conference on Learning Representations*, 2019.

[30] Zhichao Lu, Ian Whalen, Vishnu Boddeti, Yashesh Dhebar, Kalyanmoy Deb, Erik Goodman, and Wolfgang Banzhaf. NSGA-Net: neural architecture search using multi-objective genetic algorithm. In *Proceedings of the Genetic and Evolutionary Computation Conference*, 2019.

[31] Ningning Ma, Xiangyu Zhang, Hai-Tao Zheng, and Jian Sun. Shufflenet v2: Practical guidelines for efficient cnn architecture design. In *Proceedings of the European Conference on Computer Vision*, 2018.

[32] Christopher Manning and Hinrich Schutze. *Foundations of statistical natural language processing*. MIT press, 1999.

[33] Hector Mendoza, Aaron Klein, Matthias Feurer, Jost Tobias Springenberg, and Frank Hutter. Towards automatically-tuned neural networks. In *Proceedings of the Workshop on Automatic Machine Learning*. PMLR, 2016.

[34] Risto Miikkulainen, Jason Liang, Elliot Meyerson, Aditya Rawal, Dan Fink, Olivier Francon, Bala Raju, Hormoz Shahrzad, Arshak Navruzyan, Nigel Duffy, et al. Evolving deep neural networks. In *Artificial Intelligence in the Age of Neural Networks and Brain Computing*, pages 269–287. Elsevier, 2024.

[35] Hieu Pham, Melody Guan, Barret Zoph, Quoc Le, and Jeff Dean. Efficient neural architecture search via parameters sharing. In *International Conference on Machine Learning*, 2018.

[36] Ilija Radosavovic, Justin Johnson, Saining Xie, Wan-Yen Lo, and Piotr Dollár. On network design spaces for visual recognition. In *Proceedings of the IEEE/CVF International Conference on Computer Vision*, 2019.

[37] Prajit Ramachandran, Barret Zoph, and Quoc V Le. Searching for activation functions. *arXiv preprint arXiv:1710.05941*, 2017.

[38] Esteban Real, Sherry Moore, Andrew Selle, Saurabh Saxena, Yutaka Leon Suematsu, Jie Tan, Quoc V Le, and Alexey Kurakin. Large-scale evolution of image classifiers. In *International Conference on Machine Learning*, 2017.

[39] Esteban Real, Alok Aggarwal, Yanping Huang, and Quoc V Le. Regularized evolution for image classifier architecture search. In *Proceedings of the AAAI Conference on Artificial Intelligence*, 2019.

[40] Esteban Real, Chen Liang, David So, and Quoc V Le. AutoML-zero: Evolving machine learning algorithms from scratch. In *International Conference on Machine Learning*, 2020.

[41] Pengzhen Ren, Yun Xiao, Xiaojun Chang, Po-Yao Huang, Zhihui Li, Xiaojiang Chen, and Xin Wang. A comprehensive survey of neural architecture search: Challenges and solutions. *ACM Computing Surveys (CSUR)*, 54(4):1–34, 2021.

[42] Nicholas Roberts, Mikhail Khodak, Tri Dao, Liam Li, Christopher Ré, and Ameet Talwalkar. Rethinking neural operations for diverse tasks. *Advances in Neural Information Processing Systems*, 2021.

[43] Alex Rogozhnikov. Einops: Clear and reliable tensor manipulations with einstein-like notation. In *International Conference on Learning Representations*, 2022.

[44] Robin Ru, Pedro Esperanca, and Fabio Maria Carlucci. Neural architecture generator optimization. *Advances in Neural Information Processing Systems*, 2020.

[45] Simon Schrodi, Danny Stoll, Binxin Ru, Rhea Sukthanker, Thomas Brox, and Frank Hutter. Construction of hierarchical neural architecture search spaces based on context-free grammars. *Advances in Neural Information Processing Systems*, 2024.

[46] David So, Wojciech Mañke, Hanxiao Liu, Zihang Dai, Noam Shazeer, and Quoc V Le. Primer: Searching for efficient transformers for language modeling. In *Advances in Neural Information Processing Systems*, 2021.

[47] Jost Tobias Springenberg, Alexey Dosovitskiy, Thomas Brox, and Martin Riedmiller. Striving for Simplicity: The All Convolutional Net. In *ICLR Workshops*, 2015.

[48] Christian Szegedy, Wei Liu, Yangqing Jia, Pierre Sermanet, Scott Reed, Dragomir Anguelov, Dumitru Erhan, Vincent Vanhoucke, and Andrew Rabinovich. Going deeper with convolutions. In *Proceedings of the IEEE Conference on Computer Vision and Pattern Recognition*, 2015.

[49] Mingxing Tan and Quoc V Le. Mixconv: Mixed depthwise convolutional kernels. In *Proceedings of the British Machine Vision Conference*, 2019.

[50] Mingxing Tan, Bo Chen, Ruoming Pang, Vijay Vasudevan, Mark Sandler, Andrew Howard, and Quoc V Le. MnasNet: Platform-aware neural architecture search for mobile. In *Proceedings of the IEEE/CVF Conference on Computer Vision and Pattern Recognition*, 2019.

[51] Ilya Tolstikhin, Neil Houlsby, Alexander Kolesnikov, Lucas Beyer, Xiaohua Zhai, Thomas Unterthiner, Jessica Yung, Andreas Steiner, Daniel Keysers, Jakob Uszkoreit, Mario Lucic, and Alexey Dosovitskiy. MLP-Mixer: An all-MLP Architecture for Vision. In *Advances in Neural Information Processing Systems*, 2021.

[52] Hugo Touvron, Piotr Bojanowski, Mathilde Caron, Matthieu Cord, Alaaeldin El-Nouby, Edouard Grave, Gautier Izacard, Armand Joulin, Gabriel Synnaeve, Jakob Verbeek, and Hervé Jégou. ResMLP: Feedforward Networks for Image Classification With Data-Efficient Training. *IEEE Transactions on Pattern Analysis and Machine Intelligence*, 45(4):5314–5321, 2023.

[53] Renbo Tu, Nicholas Roberts, Mikhail Khodak, Junhong Shen, Frederic Sala, and Ameet Talwalkar. NAS-Bench-360: Benchmarking Neural Architecture Search on Diverse Tasks. In *Neural Information Processing Systems Datasets and Benchmarks Track*, 2022.

[54] Ashish Vaswani, Noam Shazeer, Niki Parmar, Jakob Uszkoreit, Llion Jones, Aidan N. Gomez, Łukasz Kaiser, and Illia Polosukhin. Attention is all you need. In *Advances in Neural Information Processing Systems*, 2017.

[55] Xingchen Wan, Binxin Ru, Pedro M Esperança, and Zhenguo Li. On redundancy and diversity in cell-based neural architecture search. In *International Conference on Learning Representations*, 2022.

[56] Colin White, Willie Neiswanger, and Yash Savani. BANANAS: Bayesian optimization with neural architectures for neural architecture search. In *Proceedings of the AAAI Conference on Artificial Intelligence*, 2021.

[57] Colin White, Mahmoud Safari, Rhea Sukthanker, Binxin Ru, Thomas Elsken, Arber Zela, Debadeepa Dey, and Frank Hutter. Neural Architecture Search: Insights from 1000 papers. *arXiv preprint arXiv:2301.08727*, 2023.

[58] Yuhui Xu, Lingxi Xie, Xiaopeng Zhang, Xin Chen, Guo-Jun Qi, Qi Tian, and Hongkai Xiong. Pc-darts: Partial channel connections for memory-efficient architecture search. In *International Conference on Learning Representations*, 2020.

[59] Shangshang Yang, Xiaoshan Yu, Ye Tian, Xueming Yan, Haiping Ma, and Xingyi Zhang. Evolutionary neural architecture search for transformer in knowledge tracing. *Advances in Neural Information Processing Systems*, 2023.

- [60] Chris Ying, Aaron Klein, Eric Christiansen, Esteban Real, Kevin Murphy, and Frank Hutter. Nas-bench-101: Towards reproducible neural architecture search. In *International Conference on Machine Learning*, 2019.
- [61] Kaicheng Yu, Christian Sciuto, Martin Jaggi, Claudiu Musat, and Mathieu Salzmann. Evaluating the search phase of neural architecture search. In *International Conference on Learning Representations*, 2020.
- [62] Sergey Zagoruyko and Nikos Komodakis. Wide Residual Networks. In *Proceedings of the British Machine Vision Conference*, 2016.
- [63] Xingbang Zhang, Zehao Huang, Naiyan Wang, Shiming Xiang, and Chunhong Pan. You only search once: Single shot neural architecture search via direct sparse optimization. *IEEE Transactions on Pattern Analysis and Machine Intelligence*, 43(9):2891–2904, 2020.
- [64] Zhao Zhong, Junjie Yan, Wei Wu, Jing Shao, and Cheng-Lin Liu. Practical block-wise neural network architecture generation. In *Proceedings of the IEEE/CVF Conference on Computer Vision and Pattern Recognition*, 2018.
- [65] Yuan Zhou, Haiyang Wang, Shuwei Huo, and Boyu Wang. Hierarchical full-attention neural architecture search based on search space compression. *Knowledge-Based Systems*, 269:110507, 2023.
- [66] Barret Zoph and Quoc V Le. Neural architecture search with reinforcement learning. In *International Conference on Learning Representations*, 2017.
- [67] Barret Zoph, Vijay Vasudevan, Jonathon Shlens, and Quoc V Le. Learning transferable architectures for scalable image recognition. In *Proceedings of the IEEE/CVF Conference on Computer Vision and Pattern Recognition*, 2018.

## A Search Space Details

### A.1 Sampling

In this section, we explain the process of sampling an architecture from our parameterised PCFG through an example. We specifically focus on how the running example from the main paper, a simple convolutional block with a skip connection, could be generated.

We begin the process with the starting symbol  $S$ , which could produce several forms based on the production rules, including  $(MM)$ ,  $(BMA)$ , or  $(R1MR2)$ . Since our block includes a skip connection, the macro structure of our architecture is best represented by a branching module  $(BMA)$ .

Within this module, we expand the string from left to right, thereby starting with  $(B)$ . The specific branching operation that fits our goal is  $(B \rightarrow \text{clone})$  as we wish to later combine a transformed version of the tensor with itself. Since we have two branches, they are produced separately (see branching prior) and our module becomes  $(B M_1 M_2 A)$ .

For the first branch,  $(M_1)$ , we need a set of components that constitute a convolution followed by batch normalisation and an activation. Since this involves several composed operations we first expand into a sequential module  $(M_1 \rightarrow M_3 M_4)$ . The first of these operations represents the convolution. Within `einspace`, a convolution,  $\text{conv}(x)$ , is decomposed into the three operations,  $\text{col2im}(\text{linear}(\text{im2col}(x)))$ . Thus, in our grammar we unfold it as a routing module,  $(M_3 \rightarrow R1 M_5 R2)$  which further produces  $(R1 \rightarrow \text{im2col})$ ,  $(M_5 \rightarrow C \rightarrow \text{linear})$  and  $(R2 \rightarrow \text{col2im})$ . The normalisation and activation are then generated under  $(M_4)$ , defined as another sequential module  $(M_4 \rightarrow M_6 M_7)$  with  $(M_6 \rightarrow C \rightarrow \text{norm})$  and  $(M_7 \rightarrow C \rightarrow \text{relu})$ . The second branch,  $M_2$ , acts as a skip connection and is thus derived as  $(M_2 \rightarrow C \rightarrow \text{identity})$ .

To finalise the architecture, the aggregation symbol  $(A)$  merges the tensors back into one unit. To complete the residual connection, we use the rule  $(A \rightarrow \text{add})$ .

The full derivation tree in this example is shown in Figure 3 of the main paper. This general sampling process allows the creation of complex neural network architectures from a structured and interpretable set of rules.

### A.2 Fundamental Operations

Our grammar in the main paper is somewhat simplified. There are some fundamental operations that have hyperparameters that allow multiple versions to be chosen from. They are detailed here.

**Branching functions.** For the production rule  $(B \rightarrow \text{clone} \mid \text{group-dim})$ , the full set of options is:

$$B \rightarrow \text{clone}(b=2) \mid \text{clone}(b=4) \mid \text{clone}(b=8) \mid \quad (10)$$

$$\text{group-dim(dim=1, b=2)} \mid \text{group-dim(dim=1, b=4)} \mid \text{group-dim(dim=1, b=8)} \mid \quad (11)$$

$$\text{group-dim(dim=2, b=2)} \mid \text{group-dim(dim=2, b=4)} \mid \text{group-dim(dim=2, b=8)} \mid \quad (12)$$

$$\text{group-dim(dim=3, b=2)} \mid \text{group-dim(dim=3, b=4)} \mid \text{group-dim(dim=3, b=8)}, \quad (13)$$

where  $b$  refers to the branching factor and  $\text{dim}$  is the dimension we group over.

**Aggregation functions.** Similarly, for the production rule  $(A \rightarrow \text{matmul} \mid \text{add} \mid \text{concat})$ , the full set of options is:

$$A \rightarrow \text{matmul(scaled=False)} \mid \text{matmul(scaled=True)} \mid \text{add} \mid \quad (14)$$

$$\text{concat(dim=1, b=2)} \mid \text{concat(dim=1, b=4)} \mid \text{concat(dim=1, b=8)} \mid \quad (15)$$

$$\text{concat(dim=2, b=2)} \mid \text{concat(dim=2, b=4)} \mid \text{concat(dim=2, b=8)} \mid \quad (16)$$

$$\text{concat(dim=3, b=2)} \mid \text{concat(dim=3, b=4)} \mid \text{concat(dim=3, b=8)}, \quad (17)$$

where `scaled=True` makes the `matmul` operation equivalent to the scaled dot product used in many transformer architectures,  $\text{dim}$  is the dimension we concatenate over and  $b$  is the branching factor.

**Routing functions.** The `im2col` and `col2im` functions are implemented to offer the standard functionality that enables convolutional operations, including variables that set the kernel sizes, stride, dilation and padding. Below are the full set of options for `im2col`. The `col2im` only takes the predicted output

shape as a parameter so we can include only a single version of this operation.

$$\text{im2col}(k=1, s=1, p=0), \quad \text{im2col}(k=1, s=2, p=0), \quad (18)$$

$$\text{im2col}(k=3, s=1, p=1), \quad \text{im2col}(k=3, s=2, p=1), \quad (19)$$

$$\text{im2col}(k=4, s=4, p=0), \quad \text{im2col}(k=8, s=8, p=0), \quad \text{im2col}(k=16, s=16, p=0), \quad (20)$$

where  $k$  is the kernel size,  $s$  is the stride and  $p$  the padding.

For the permute operation, there are 6 versions of the order parameter  $o$ . There is one for the Col mode and 5 for the Im mode:

$$\text{permute}(o=(2,1)), \quad (21)$$

$$\text{permute}(o=(1,3,2)), \quad \text{permute}(o=(2,1,3)), \quad \text{permute}(o=(2,3,1)), \quad (22)$$

$$\text{permute}(o=(3,1,2)), \quad \text{permute}(o=(3,2,1)). \quad (23)$$

For completeness, the identity operation can also be included, making 2 in the Col mode (with  $\text{identity}=\text{permute}(o=(1,2))$ ) and 6 in the Im mode (with  $\text{identity}=\text{permute}(o=(1,2,3))$ ).

**Computation functions.** For linear layers, we vary the output dimension  $d$  across powers of two:

$$\text{linear}(d=16), \quad \text{linear}(d=32), \quad \text{linear}(d=64), \quad (24)$$

$$\text{linear}(d=128), \quad \text{linear}(d=256), \quad \text{linear}(d=512), \quad (25)$$

$$\text{linear}(d=1024), \quad \text{linear}(d=2048). \quad (26)$$

The `norm` operation takes on the `batch-norm` functionality in the Im mode and `layer-norm` in Col mode. The `softmax` is just a softmax operation applied to the final dimension, the `relu` activation is implemented as the single option `leaky-relu` and `pos-enc` is a learnable positional encoding.

### A.3 Patch Embeddings and Convolutions

In this section we provide some more information about how the routing module can represent common components.

The routing module, ( $M \rightarrow R1 M R2$ ), puts a prior on certain types of operations inside our architectures. A patch embedding, such as those found in many transformers, is achieved by the following derivation: ( $M \rightarrow \text{im2col linear identity}$ ), while a convolution can be obtained by ( $M \rightarrow \text{im2col linear col2im}$ ). In terms of the process required to sample such combinations, the first is easy since there are no dependencies between the operations. The second, however, is more complicated and requires some discussion.

Let  $x$  be a tensor in  $\mathbb{R}^{3 \times 32 \times 32}$  and let's consider a routing module containing the functions: `im2col`, `linear`, `col2im`. The functions will be applied in order to the input tensor, giving us

$$x' = \text{im2col}(x), \quad (27)$$

$$x'' = \text{linear}(x'), \quad (28)$$

$$y = \text{col2im}(x''). \quad (29)$$

The shapes of the intermediate and final tensors  $\{x', x'', y\}$  depend on several function hyperparameters. These are listed below.

Table 2: Hyperparameters for the three functions involved in a convolution component.

<code>im2col</code>	<code>col2im</code>	<code>linear</code>
$k_{in} = 7$ (kernel size)	$k_{out} = 7$ (kernel size)	$c_{out} = 64$ (output channels)
$s_{in} = 2$ (stride)	$s_{out} = 2$ (stride)	
$p_{in} = 3$ (padding)	$p_{out} = 0$ (padding)	

The input tensor has height dimension  $h_{in}$  and width  $w_{in}$ . The `im2col` operation will extract column vectors from this space a number of times depending on the kernel size  $k_{in}$ , stride  $s_{in}$  and padding  $p_{in}$  values in the table above. The number of column vectors equals

$$l = \left\lfloor \frac{h_{in} + 2 \times p_{in} - (k_{in} - 1) - 1}{s_{in}} + 1 \right\rfloor \times \left\lfloor \frac{w_{in} + 2 \times p_{in} - (k_{in} - 1) - 1}{s_{in}} + 1 \right\rfloor, \quad (30)$$

which in our case gives  $l = 256$ . The shapes of all intermediate tensors can therefore be written as in Table 3.

Table 3: Tensor shapes in the forward pass of our convolution component.  $c_{in} = 3, h_{in} = 32, w_{in} = 32$  in this example.

Tensor	Shape
$x$	$[c_{in}, h_{in}, w_{in}]$
$x'$	$[l, c_{in} \times k_{in} \times k_{in}]$
$x''$	$[l, c_{out}]$
$y$	$[c_{out}, h_{out}, w_{out}]$

Therefore, to successfully apply the `col2im` function, the constraint  $l = h_{out} \times w_{out}$  must be satisfied. From Equation 30 we can see that the output height and width can be predicted by the `im2col` parameters.

$$h_{out} = \left\lfloor \frac{h_{in} + 2 \times p_{in} - (k_{in} - 1) - 1}{s_{in}} + 1 \right\rfloor \quad (31)$$

$$w_{out} = \left\lfloor \frac{w_{in} + 2 \times p_{in} - (k_{in} - 1) - 1}{s_{in}} + 1 \right\rfloor \quad (32)$$

So, in practice, the `im2col` operation fully defines the behaviour of the convolution—apart from the number of output channels defined by the linear layer—and the `col2im` only rearranges the tensor back into its correct 3D form. This is trivial in the case where  $h_{in} = w_{in}$  since  $h_{out} = w_{out} = \sqrt{l}$ . However, if  $h_{in} \neq w_{in}$ , then the predicted output shapes must be remembered until the `col2im` operation is applied.

Thus, in our sampling and mutation algorithm, whenever an `im2col` operation is sampled, we must store the predicted output shape until a corresponding `col2im` is applied. Additionally, the dimensionality of  $l$  must not change in the connecting branch as it would break the constraint  $h_{out} = w_{out} = \sqrt{l}$ .

#### A.4 Branching Rate of the CFG

If a PCFG is consistent, the probabilities of all finite derivations sum to one, or equivalently, it has a zero probability of generating infinite strings or derivations. For us, that means a sampled architecture can not be infinitely large, and that the sampling algorithm will halt with probability one. In order to check if a CFG is consistent, we can inspect the spectral radius  $\rho$  of its non-terminal expectation matrix [8]. If  $\rho < 1$ , then the PCFG is consistent. This expectation matrix is indexed by the non-terminals in the grammar (both the columns and the rows), and at each cell it provides the expected number of instances the column non-terminal being generated from the row non-terminal by summing the probabilities of the row non-terminal multiplied by the count of the column non-terminal in each rule.

We can also solve a (simple, in our case) set of linear equations in order to compute the expected length of an architecture string,  $\ell$ , as a function of the rule probabilities. More specifically, denote by  $\mathbb{E}[A]$  the expected length of string generated by a nonterminal in the grammar  $A$ . Then  $\ell = \mathbb{E}[S]$ , where:

$$\mathbb{E}[S] = \sum_{S \rightarrow \alpha} p(S \rightarrow \alpha | S) \sum_i \mathbb{E}[\alpha_i] \quad (33)$$

$$\mathbb{E}[M] = \sum_{M \rightarrow \alpha} p(M \rightarrow \alpha | M) \sum_i \mathbb{E}[\alpha_i] \quad (34)$$

$$\mathbb{E}[B] = 1 \quad (35)$$

$$\mathbb{E}[A] = 1 \quad (36)$$

$$\mathbb{E}[R1] = 1 \quad (37)$$

$$\mathbb{E}[R2] = 1 \quad (38)$$

$$\mathbb{E}[C] = 1 \quad (39)$$

In the above,  $\alpha$  is the right hand side of a rule and  $\alpha_i$  varies over the nonterminals in that right hand side.

## B Implementation and Experimental Details

### B.1 Networks

#### Baseline networks

We use the convolutional baselines of ResNet18 [19] and WideResNet-16-4 [62]. Both stems use a  $3 \times$  convolution instead of the standard  $7 \times 7$  as most input shapes in the datasets we use are small. The former contains a max-pooling layer in the stem, which for simplicity we decide to not represent in our search space. Instead we modify the pooling operation and replace it with a  $3 \times$  convolution with stride 2. This has been shown to be equally powerful [47] and in our experiments we find that it performs similarly. Our ViT model is a small 4-layer network with a patch size of 4, model width of 512, and 4 heads. The MLP-Mixer shares the same patch embedding stem with a patch size of 4. It has 8 layers and, similarly, a model width of 512. The channel mixer expands the dimension by 4 and the token mixer cuts it in half. The models have the following number of parameters (given an input image of shape [3, 64, 64]): Resnet18: 11.2M, WRN16-4: 2.8M, ViT: 4.4M and MLP-Mixer: 6.5M.

#### Network head

Every network that is instantiated contains a few common operations. For classification tasks, the network head takes the following form: the output features of the sampled backbone are reduced to their channel dimension via `reduce('B C H W -> B C', 'mean')` or `reduce('B C H -> B C', 'mean')`, depending on if the features are in `Im` or `Co1` mode. Second, a final linear layer that maps the channel dimension to the target dimension (i.e., the number of classes) is appended. For dense prediction tasks: the head contains an adaptive average pooling layer that upsamples the two final dimensions of the backbone features to the target image size. If the features are in the `Co1` mode, we insert a new dimension after the batch size. Then regardless of mode, a linear layer adjusts the number of channels to the target channel number.

#### Network training

Each network is trained and evaluated separately with no weight sharing. During the search phase we minimise the loss on a train split and compute the validation metric on a validation set. To evaluate the final chosen module, we retrain on `train+val` splits and evaluate on test. To speed up our experiments, the inner loop optimisation of architectures uses fewer epochs compared to the evaluation phase. All networks are trained using the SGD optimizer with momentum of 0.9. The values for learning rate, weight decay, batch size and more can be found in Table 4.

Table 4: Hyperparameters for each dataset.

Dataset name	Metric type	Baseline model	Epochs (search)	Epochs (eval)	Batch size	Learning rate	Weight decay	Momentum
AddNIST	Accuracy	ResNet18	8	64	256	0.04	$3 \times 10^{-4}$	0.9
Language	Accuracy	ResNet18	8	64	256	0.04	$3 \times 10^{-4}$	0.9
MultNIST	Accuracy	ResNet18	8	64	256	0.04	$3 \times 10^{-4}$	0.9
CIFARTile	Accuracy	ResNet18	8	64	256	0.04	$3 \times 10^{-4}$	0.9
Gutenberg	Accuracy	ResNet18	8	64	256	0.04	$3 \times 10^{-4}$	0.9
Isabella	Accuracy	ResNet18	8	64	256	0.04	$3 \times 10^{-4}$	0.9
GeoClassing	Accuracy	ResNet18	8	64	256	0.04	$3 \times 10^{-4}$	0.9
Chesseraact	Accuracy	ResNet18	8	64	256	0.04	$3 \times 10^{-4}$	0.9
CIFAR100	0-1 error	WRN16-4	25	200	128	0.1	$5 \times 10^{-4}$	0.9
Spherical	0-1 error	WRN16-4	25	200	128	0.1	$5 \times 10^{-4}$	0.9
NinaPro	0-1 error	WRN16-4	25	200	128	0.1	$5 \times 10^{-4}$	0.9
Darcy Flow	relative $\ell_2$	WRN16-4	25	200	4	0.001	$5 \times 10^{-4}$	0.9
Cosmic	1 - AUROC	WRN16-4	25	200	8	0.001	$5 \times 10^{-4}$	0.9

### B.2 Datasets

We followed the official instructions of Unseen NAS [16] to setup the datasets. Descriptions of each dataset follow:

#### AddNIST

This dataset is derived from the MNIST dataset. Specifically, each RGB image is computed by

stacking three MNIST images in the channel dimension. Each image has the shape  $3 \times 28 \times 28$ . It has a total of 20 categories; the class label is computed by summing the MNIST labels in all three channels. Among the 70,000 images, 45,000 are used for training, 15,000 are used for validation, and 10,000 images are used for testing.

### **Language**

Language consists of six-letter words extracted from dictionaries of ten Latin alphabet languages: English, Dutch, German, Spanish, French, Portuguese, Swedish, Zulu, Swahili, and Finnish. Words containing diacritics or the letters ‘y’ and ‘z’ are excluded, making an alphabet of 24 letters. Each sample consists of four words encoded into a binary image of shape  $1 \times 24 \times 24$ . The task is to predict the language of the sample. Along the y-axis are the letter positions in the concatenated 24-letter string, and along the x-axis are the letters in the alphabet. As an example, a one in the position (0, 0) indicates that the first letter in the string is an ‘a’. The dataset is split into 50,000 training samples, 10,000 validation samples, and 10,000 test samples.

### **MultNIST**

MultNIST is a dataset designed similarly to AddNIST, originating from the same research objective. Each channel of the 3 channel images contains an image from the MNIST dataset. Each image has the shape  $3 \times 28 \times 28$ . The dataset is divided into 50,000 training images, 10,000 validation images, and 10,000 test images. Unlike AddNIST, MultNIST comprises ten classes (0-9), the label for each MultNIST image is computed using the formula  $l = (r \times g \times b) \bmod 10$ , where  $r$ ,  $g$  and  $b$  are the MNIST labels of the red, green, and blue channels, respectively.

### **CIFARTile**

CIFARTile is a dataset where each image is a composite of four CIFAR-10 images arranged in a  $2 \times 2$  grid, making each sample an image of shape  $3 \times 64 \times 64$ . The dataset is divided into 45,000 training images, 15,000 validation images, and 10,000 test images. CIFARTile has four classes (0-3), determined by the number of distinct CIFAR-10 classes in each grid, minus one.

### **Gutenberg**

Gutenberg is a dataset sourced from Project Gutenberg. It includes texts from six authors, with basic text preprocessing applied: punctuation removal, diacritic conversion, and elimination of structural words. The dataset contains consecutive sequences of three words (3-6 letters each), padded to 6 characters and concatenated into 18-character strings. These strings are converted into images with size  $1 \times 27 \times 18$ , with the x-axis representing character positions and the y-axis representing alphabetical letters or spaces. The task is to predict the author of each sequence. The dataset is split into 45,000 training, 15,000 validation, and 6,000 test images.

### **Isabella**

Isabella is a dataset derived from musical recordings of the Isabella Stewart Gardner Museum, Boston. It includes four classes based on the era of composition: Baroque, Classical, Romantic, and 20th Century. The recordings are split into five-second snippets and converted into 64-band spectrograms, resulting in images with dimensions  $1 \times 64 \times 128$ . The dataset is divided into 50,000 training images, 10,000 validation images, and 10,000 test images, ensuring no overlap of recordings across splits. The task is to predict the era of composition from the spectrogram.

### **GeoClassing**

GeoClassing is based on the BigEarthNet dataset. It uses satellite images initially labeled for ground-cover classification but reclassified by the European country they depict. The dataset includes ten classes: Austria, Belgium, Finland, Ireland, Kosovo, Lithuania, Luxembourg, Portugal, Serbia, and Switzerland. Each image is of size  $3 \times 64 \times 64$ . The dataset is split into 43,821 training images, 8,758 validation images, and 8,751 test images. The task is to predict the country depicted in each image based on topology and ground coverage.

### **Chesseract**

Chesseract is a dataset derived from public chess games of eight grandmasters. The dataset consists of the final 15% of board states from these games. Each position is one-hot encoded by piece type and color, resulting in  $1 \times 8 \times 8$  images. The dataset is divided into 49,998 training images, 9,999 validation images, and 9,999 test images, ensuring no positions from the same game appear across splits. Each image is classified into one of three classes: White wins, Draw, or Black wins. The

Table 5: Lower is better. Our results from performing random sampling, random search and regularised evolution in `einspace` on NASBench360 [53]. We compare to the results from [53], where the DARTS search space is used. RE(WRN) refers to initialising the regularised evolution search algorithm with WRN architecture. **Best** and second best performance per dataset.

	WRN	DARTS (GAEA)	Expert	RE(WRN) <code>einspace</code>
CIFAR100	25.61	24.02	<b>19.39</b>	<u>21.47</u>
Spherical	76.32	<b>48.23</b>	67.41	<u>66.37</u>
NinaPro	10.32	17.67	<u>8.73</u>	<b>6.37</b>
Darcy Flow	0.032	0.026	<b>0.008</b>	<u>0.014</u>
Cosmic	0.245	<u>0.229</u>	<b>0.127</b>	0.73
Average rank ↓	3.60	2.60	<b>1.60</b>	<u>2.20</u>

task is to predict the game’s result based on the given board position. We pad the input with 5 zero-valued pixels to make a  $12 \times 18 \times 18$  tensor.

We follow the official instructions of NASBench360 [53] to setup the datasets. Dataset descriptions follow (noting that we are using a subset of all the datasets):

#### CIFAR100

CIFAR100 is a widely known image classification dataset with 100 fine-grained classes. Each image is of size  $3 \times 32 \times 32$ . The dataset is split into 40,000 training, 10,000 validation and 10,000 testing images. We preprocess the images by applying random crops, horizontal flips, and normalisation.

#### Spherical

Spherical dataset consists on classifying spherically projected CIFAR100 images. Specifically, CIFAR images are projected to the northern hemisphere with a random rotation. Each image is of size  $3 \times 60 \times 60$ . Spherical dataset uses the same split ratios as CIFAR100. In this case, there is no data augmentation nor pre-processing steps.

#### NinaPro

NinaPro is a dataset for classifying hand gestures given their electromyography signals. EMG data signals are collected with two Myo armbands as wave signals. Wave signals, along with their wavelength and frequency, are processed 2D signals of shape  $1 \times 16 \times 52$ . There are 18 classes, which are heavily imbalanced, with the neutral position amounting for 65% of all gestures. The dataset is split into 2,638 training samples, 659 validation samples, and 659 testing samples. No further data augmentation is applied.

#### Darcy Flow

Darcy Flow is a regression task for predicting the solution of a 2D PDE at a predefined later stage given some 2D initial conditions. The input is a  $1 \times 85 \times 85$  image describing the initial state of the fluid. The output should match the same dimensions. The dataset is split into 900 images for training, 100 for validation, and 100 for test. Input data is normalised.

#### Cosmic

Cosmic contains images from the F435W filter collected from the Hubble Space Telescope. It aims to identify cosmic rays (corrupted pixels) in the images. Inputs are images of  $1 \times 256 \times 256$ , and outputs are pixel binary predictions (artifact vs. no-artifact). The dataset is split into 4,347 images for training, 483 for validation, and 420 for test.

### B.3 Compute Resources

All our experiments ran on our two internal clusters with the following infrastructure:

- AMD EPYC 7552 48-Core Processor with 1000GB RAM and 8× NVIDIA RTX A5500 with 24GB of memory
- AMD EPYC 7452 32-Core Processor with 400GB RAM and 7× NVIDIA A100 with 40GB of memory

Table 6: The distribution of terminal and nonterminal symbols as well as average branching factors in 2000 sampled architectures with varying values for the computation module probability  $p(M \rightarrow C | M)$ . For probability values 0.2 and 0.1 there is no data, as the sampling process is too time-consuming.

Type	$p(M \rightarrow C   M)$	Min	Mean	Median	Std	Max
terminals	0.9	2	3.87	3.00	2.84	28
	0.8	2	5.34	4.00	6.32	54
	0.7	2	6.72	4.00	11.22	118
	0.6	2	8.65	4.00	16.73	202
	0.5	2	40.22	5.00	303.65	4779
	0.4	2	100.15	8.00	749.61	12026
	0.3	2	6070.77	9.00	64863.45	878122
non-terminals	0.9	2	3.63	3.00	3.45	42
	0.8	2	5.04	3.00	6.91	64
	0.7	2	6.00	3.00	9.21	81
	0.6	2	7.74	4.00	13.61	165
	0.5	2	39.03	5.00	325.18	5219
	0.4	2	88.58	8.00	649.44	10417
	0.3	2	4588.13	8.00	50203.87	734497
branching factor	0.9	1	1.75	1.00	1.63	7.61
	0.8	1	2.05	1.00	1.95	7.73
	0.7	1	2.05	1.00	1.91	7.83
	0.6	1	2.17	1.00	1.96	7.73
	0.5	1	2.34	1.00	2.00	7.88
	0.4	1	2.81	1.75	2.14	7.87
	0.3	1	2.80	1.75	2.13	7.96

Each experiment used a single GPU to train each architecture. Running 1000 iterations of RE(Scratch) on the quickest datasets (Language and Chesseract) took around 2 days, while the slowest (GeoClassing) took 4 days. We had very similar training times for RE(RN18) and RE(Mix) which ran for 500 iterations.

## C Additional Results

### C.1 NAS-Bench-360

We test `einspace` on a selection of datasets from NAS-Bench-360 [53] to further showcase its potential. These results can be found in Table 5. In this setting the baseline network is a WideResNet-16-4 (WRN). We see that our regularised evolution with the baseline as the initial seed, RE(WRN), again consistently finds architectural improvements. It also outperforms the GAEA search strategy on the DARTS search space on all but the Cosmic task. On NinaPro, it even beats the Expert architecture, specifically designed for this task. Note that the WRN baseline network on its own does not achieve as low an error as reported in [53]. However, our `einspace` architecture beats even this number and to the best of our knowledge sets a new state-of-the-art.

### C.2 Empirical Architecture Complexity

For our experiments we set the computation module probability to  $p(M \rightarrow C | M) = 0.32$  using the branching rate method described in A.4. We now report some empirical results for the architecture complexities as we vary this value. In Table 6 we can see that the complexity, as measured by the count of terminals and non-terminals in the derivation trees, grows as the probability decreases.

When searching for an architecture on a new unknown task, the flexibility of the search space is key. During our random searching on `einspace` we found that we sampled networks with parameter counts ranging from zero up to 1 billion, and as few as two operations to as many as 3k. The frequency of all functions in `einspace` that appear in these networks can be found in Figure 7.

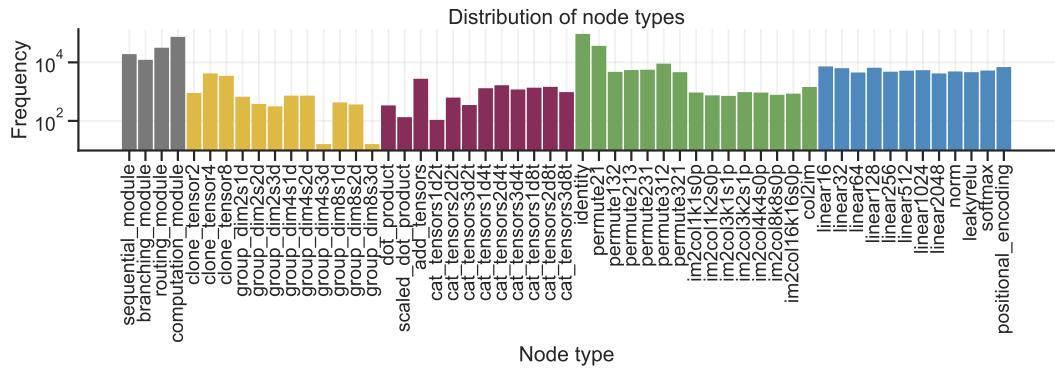


Figure 7: Frequency of each module/function in 8k sampled architectures with  $p(M \rightarrow C | M) = 0.32$ .

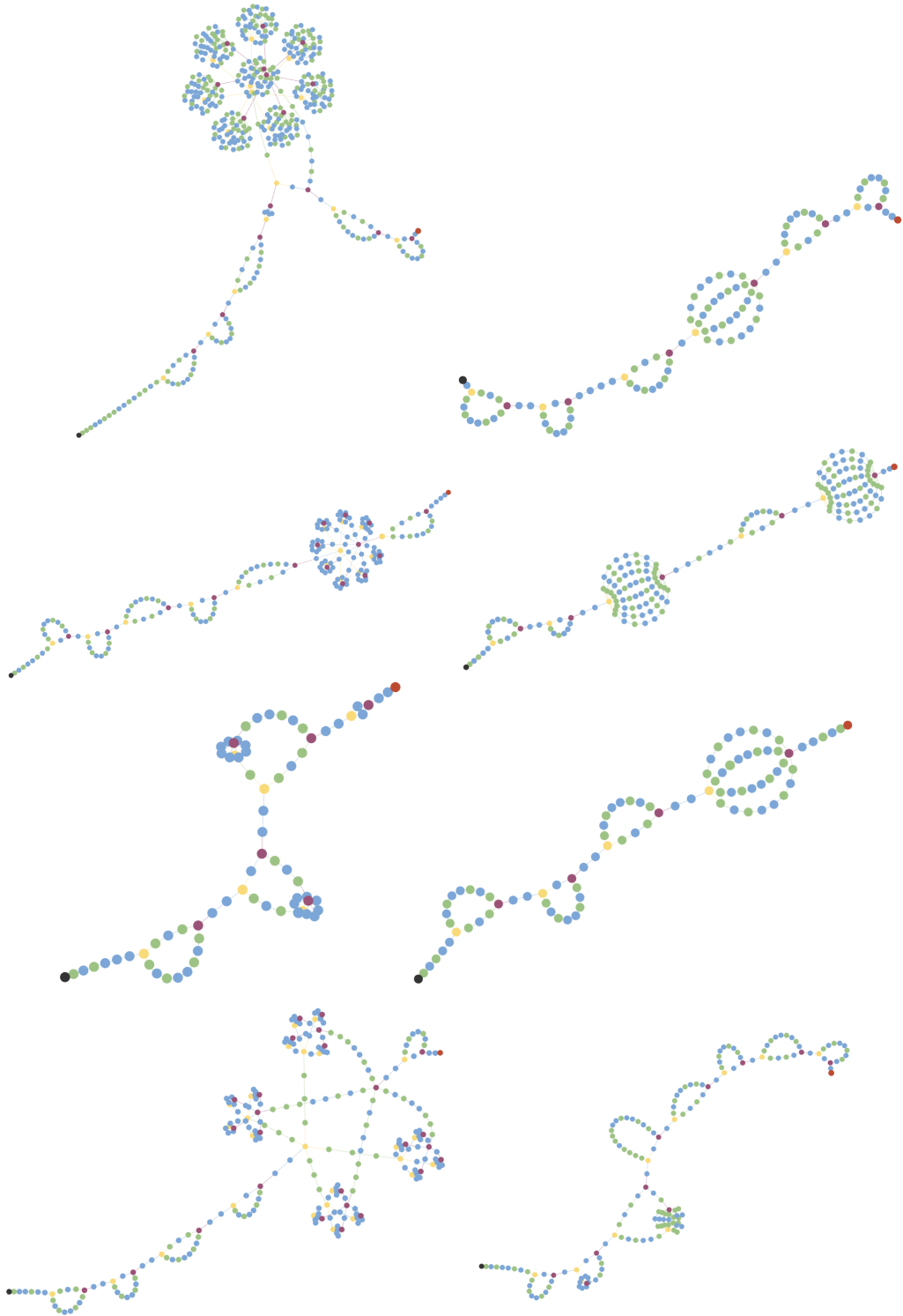


Figure 8: The top architectures found by RE(Mix) in `einspace` on Unseen NAS. From left to right, row by row: AddNIST, Language, MultNIST, CIFARTile, Gutenberg, Isabella, GeoClassing, Chesseract.